PHYSICAL REVIEW B **85**, 235420 (2012)

Probing the quantum behavior of a nanomechanical resonator coupled to a double quantum dot

Zeng-Zhao Li,[1,2] Shi-Hua Ouyang,[1,2] Chi-Hang Lam,[2] and J. Q. You[1,3,*]
[1]*Department of Physics, State Key Laboratory of Surface Physics, Fudan University, Shanghai 200433, China*
[2]*Department of Applied Physics, Hong Kong Polytechnic University, Hung Hom, Hong Kong, China*
[3]*Beijing Computational Science Research Center, Beijing 100084, China*
(Received 7 January 2012; revised manuscript received 1 April 2012; published 7 June 2012)

We propose a current correlation spectrum approach to probe the quantum behaviors of a nanomechanical resonator (NAMR). The NAMR is coupled to a double quantum dot (DQD), which acts as a quantum transducer and is further coupled to a quantum-point contact (QPC). By measuring the current correlation spectrum of the QPC, shifts in the DQD energy levels, which depend on the phonon occupation in the NAMR, are determined. Quantum behaviors of the NAMR could, thus, be observed. In particular, the cooling of the NAMR into the quantum regime could be examined. In addition, the effects of the coupling strength between the DQD and the NAMR on these energy shifts are studied. We also investigate the impacts on the current correlation spectrum of the QPC due to the backaction from the charge detector on the DQD.

DOI: 10.1103/PhysRevB.85.235420 PACS number(s): 85.85.+j, 03.67.Mn, 42.50.Lc

I. INTRODUCTION

The observation of quantum-mechanical behaviors in nanoelectromechanical systems, in particular, nanomechanical resonators (NAMRs) for testing the basic principles of quantum mechanics[1–3] has become a topic of considerable interest and activity. Besides their wide range of potential applications,[1,2] e.g., serving as ultrasensitive sensors in high-precision displacement measurements, and detection of gravitational waves, quantized NAMRs are potentially useful for quantum-information processing. For example, NAMRs may serve as a unique intermediary for transferring quantum information between microwave and optical domains because they can be coupled to electromagnetic waves of any frequency.[4]

At very low temperatures (in the milli-Kelvin range), NAMRs of high-vibration frequencies (gigahertz range) have recently been experimentally verified to approach the quantum limit.[5–11] However, low-frequency ($\lesssim$100-MHz) mechanical oscillators have the distinct advantages of high-quality factors, long phonon lifetimes, and large motional state displacements, which are important for future testing of quantum theory[12] and other applications. A formidable challenge (see, e.g., Refs. 5–10) in this field is to detect the quantum quivering (zero-point motion) of an NAMR so as to quantitatively verify whether it has been cooled into the quantum-mechanical regime or not. To directly detect the extremely small displacements of an NAMR vibrating at gigahertz frequencies by using available displacement-detection techniques is very difficult.[8–11] The usual position-measurement method is also severely limited by the "zero-point displacement" fluctuations in the quantum regime,[13] although near-Heisenberg-limited measurements have been performed in recent experiments.[14]

In this paper, we propose a current spectroscopic approach to study the behaviors of an NAMR. It is based on the detection of the current correlation spectrum in a charge detector, e.g., a quantum-point contact (QPC), which is indirectly coupled to an NAMR via a double quantum dot (DQD) acting as a quantum-electro-mechanical transducer.[15] Based on this proposal, we show that one can observe the quantum behaviors of the NAMR and can further verify whether it has been cooled into the quantum regime. In contrast to a previous approach based on the superconducting qubit coupled to a cavity, which involves Rabi splitting,[16] our proposed setup is expected to provide better tunability via the gate voltages. Moreover, we also study the effects of the backaction from the charge detector on the DQD.

We consider a coupled NAMR-DQD system in the strong *dispersive regime* where the coupling strength g is much smaller than the frequency detuning δ between the DQD and the NAMR. In this regime, energy quanta in the NAMR are only virtually exchanged between the DQD and the NAMR. Thus, the coupling of the DQD to the NAMR does not change the occupation state of the electron in the DQD, but only results in phonon-number-dependent frequency shifts in the DQD energy levels. These shifts are analogous to Stark shifts and can be further detected by measuring the current correlation spectrum of the QPC.

This paper is organized as follows. In Sec. II, the coupled system is explained. The effective dispersive Hamiltonian is derived in Sec. III. The quantum dynamics of the coupled NAMR-DQD system in the presence of the QPC are derived in Sec. IV. In Sec. V, results related to the observation of quantum behaviors, the verification of the ground-state cooling of an NAMR, as well as the backaction from the QPC on the DQD are analyzed. Conclusions are given in Sec. VI.

II. THE COUPLED NAMR-DQD-QPC SYSTEM

The device layout of an NAMR capacitively coupled to a lateral DQD, which is further measured by a QPC, is presented in Fig. 1(a). Here, we consider a Coulomb-blockade regime with strong intradot and interdot Coulomb interactions so that only one electron is allowed in the DQD. The states of the DQD are denoted by occupation states $|1\rangle$ and $|2\rangle$, representing one electron in the left and the right dots, respectively. The stereographical diagram of this device is shown in Fig. 1(b). The lateral DQD is formed by properly tuning the voltages applied to the gates. Also, an electron can be injected from the left reservoir to the DQD by changing the gate voltages. A metallic NAMR is fabricated above the DQD, and the displacement of the NAMR from its equilibrium position

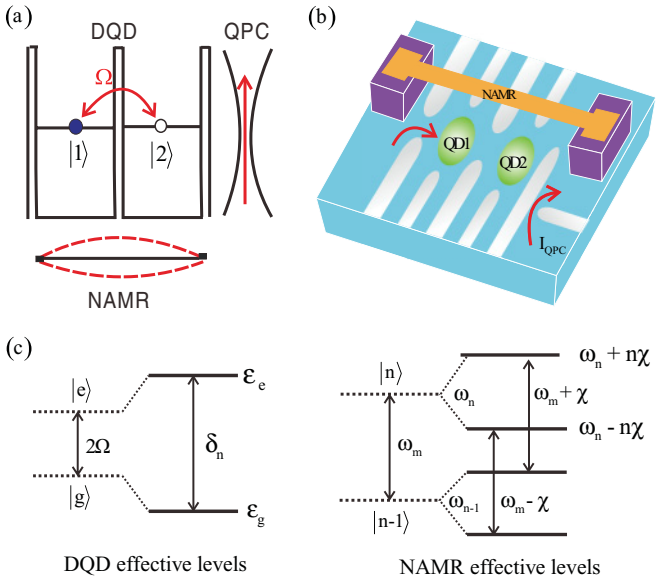

FIG. 1. (Color online) (a) Schematic of an NAMR capacitively coupled to a DQD, which is under measurement by a nearby QPC. The energy detuning between the two dot states in the DQD is zero, and the interdot coupling strength between them is Ω. (b) A stereographical diagram of the device where an electron is injected from the left reservoir to the DQD by changing the gate voltages, and the displacement of the metallic NAMR from its equilibrium position modulates the capacitance between the NAMR and the DQD. (c) Effective energy levels for the DQD (horizontal solid lines in the left panel) in the dispersive DQD-NAMR coupling regime: $\varepsilon_e = \Omega + (n+1/2)\chi$ and $\varepsilon_g = -\Omega - (n+1/2)\chi$ with energy detuning $\delta_n = 2\Omega + (2n+1)\chi$; effective energy levels for the NAMR (horizontal solid lines in the right panel) in the dispersive DQD-NAMR coupling regime: $\omega_n + n\chi$ and $\omega_n - n\chi$ with $\omega_n = n\omega_m$. The effective phonon level differences are $\omega_m + \chi$ and $\omega_m - \chi$.

modulates the mutual capacitance between the NAMR and the DQD.[17] The current $I_{\rm QPC}$ through the QPC depends on the electron occupation of the DQD.

The total Hamiltonian of the whole system is

$$H = H_{\rm sys} + H_{\rm int} + H_{\rm det}, \tag{1}$$

with an unperturbed part,

$$H_{\rm sys} = H_{\rm NAMR} + H_{\rm DQD} + H_{\rm QPC}, \tag{2}$$

where (after setting $\hbar = 1$),

$$H_{\rm NAMR} = \omega_m b^\dagger b, \tag{3}$$

$$H_{\rm DQD} = \frac{\Delta}{2}(a_2^\dagger a_2 - a_1^\dagger a_1) + \Omega(a_2^\dagger a_1 + a_1^\dagger a_2), \tag{4}$$

$$H_{\rm QPC} = \sum_k \omega_{Sk} c_{Sk}^\dagger c_{Sk} + \sum_q \omega_{Dq} c_{Dq}^\dagger c_{Dq}. \tag{5}$$

The interaction parts are

$$H_{\rm int} = -(g_2 a_2^\dagger a_2 + g_1 a_1^\dagger a_1)(b^\dagger + b), \tag{6}$$

$$H_{\rm det} = \sum_{kq}(T_0 - \zeta_2 a_2^\dagger a_2 - \zeta_1 a_1^\dagger a_1)(c_{Sk}^\dagger c_{Dq} + c_{Dq}^\dagger c_{Sk}). \tag{7}$$

Here, $H_{\rm NAMR}$, $H_{\rm DQD}$, and $H_{\rm QPC}$, respectively, are the free Hamiltonians of the NAMR, the DQD, and the QPC without the tunneling terms. The phonon operators $b^\dagger$ and b, respectively, create and annihilate an excitation of frequency ω_m in the NAMR. In Eq. (4), Δ is the energy detuning between the two dots, and Ω is the interdot coupling. Below, we consider, for simplicity, the degenerate-state case with $\Delta = 0$ [see Fig. 1(a)]. c_{Sk} (c_{Dq}) is the annihilation operator for electrons in the source (drain) reservoir of the QPC with momentum k (q). Here, we define pseudospin operators $\sigma_z \equiv a_2^\dagger a_2 - a_1^\dagger a_1$ and $\sigma_x \equiv a_2^\dagger a_1 + a_1^\dagger a_2$ with a_1 (a_2) being the annihilation operator for an electron staying at the left (right) dot. $H_{\rm int}$ is the electromechanical coupling between the NAMR and dots 1 and 2 with coupling strengths g_1 and g_2. The relative coupling strength $g \equiv (g_2 - g_1)/2$ is about $0.1\omega_m \sim 0.5\omega_m$ for typical electromechanical couplings (see, e.g., Ref. 18). $H_{\rm det}$ describes tunnelings in the QPC, which depends on the electron occupation of the DQD, owing to the electrostatic coupling between the DQD and the QPC. We define $T \equiv T_0 - (\zeta_2 + \zeta_1)/2$ and $\zeta \equiv (\zeta_2 - \zeta_1)/2$ so that the transition amplitude of the QPC when an extra electron stays at the left and right dots equals $T + \zeta$ or $T - \zeta$, respectively.

III. EFFECTIVE DISPERSIVE HAMILTONIAN

In the eigenstate basis, the DQD Hamiltonian can be written as

$$H_{\rm DQD} = \Omega\varrho_z, \tag{8}$$

where $\varrho_z = a_e^\dagger a_e - a_g^\dagger a_g$ with the two eigenstates of the DQD given by $|g\rangle = (|1\rangle - |2\rangle)/\sqrt{2}$ and $|e\rangle = (|1\rangle + |2\rangle)/\sqrt{2}$ and the energy splitting between these two eigenstates is 2Ω. Then, the total Hamiltonian becomes

$$H = \omega_m b^\dagger b + \Omega\varrho_z + g\varrho_x(b^\dagger + b) + H_{\rm QPC} + \sum_{kq}[T + \zeta\varrho_x](c_{Sk}^\dagger c_{Dq} + c_{Dq}^\dagger c_{Sk}), \tag{9}$$

where $\varrho_x = a_e^\dagger a_g + a_g^\dagger a_e$.

In the dispersive DQD-NAMR coupling regime with $|\eta| < 1$, where $\eta = g/\delta$ and $\delta = 2\Omega - \omega_m$, applying a canonical transformation $UHU^\dagger$ on the Hamiltonian (9), where $U = e^s$ with $s = \eta(\varrho_+ b - \varrho_- b^\dagger)$, one obtains an effective dispersive Hamiltonian. Under the rotating-wave approximation, this dispersive Hamiltonian can be written, up to second order in η, as $H = H_0 + H_{\rm I}$, with

$$H_0 = \omega_m b^\dagger b + \Omega\varrho_z + \chi\left(\frac{1}{2} + b^\dagger b\right)\varrho_z + H_{\rm QPC}, \tag{10}$$

$$H_{\rm I} = \sum_{kq}(T + \zeta\varrho_x)(c_{Sk}^\dagger c_{Dq} + c_{Dq}^\dagger c_{Sk}). \tag{11}$$

Here, $\chi = g^2/\delta$. The third term in Eq. (10) is a dispersive interaction that can be viewed as either a DQD-state-dependent frequency shift in the NAMR or a phonon-number-dependent shift in the DQD transition frequency. This interaction implies that, when the DQD state is excited (deexcited), an energy 2χ is effectively added to (removed from) each NAMR phonon. A similar frequency shift also appears in analogous systems in quantum optics.[19] The dispersive NAMR-DQD energy levels, described by the first three terms in Eq. (10), are the quantum version of the ac Stark effect. When there is no interaction

($g = 0$) between the NAMR and the DQD, energy differences between adjacent levels of the NAMR or the DQD are simply ω_m or 2Ω, respectively. However, for $g > 0$, these eigenstates are dressed by the dispersive interaction. The corresponding phonon level differences become $\omega_m - \chi$ for the DQD state $|g\rangle$ and $\omega_m + \chi$ for state $|e\rangle$, whereas the DQD energy split is

$$\delta_n \equiv 2\Omega + (2n+1)\chi \tag{12}$$

for phonon number n in the NAMR. Figure 1(c) shows these effective energy-level differences. The phonon-number-dependent frequency shift in the DQD as well as the DQD-state-dependent shift in the NAMR can be detected as will be explained below.

IV. QUANTUM DYNAMICS OF THE COUPLED NAMR-DQD SYSTEM

We now derive a master equation to describe the quantum dynamics of the coupled system. In the interaction picture with the dispersive Hamiltonian H_0 in Eq. (10), the interaction Hamiltonian H_I [Eq. (11)] can be written as

$$H_I(t) = S(t)Y(t), \tag{13}$$

with

$$S(t) = \sum_{j=1}^{3} P_j e^{i\widehat{\omega}_j t}, \tag{14}$$

$$Y(t) = \sum_{kq} [F_{kq}^{\dagger}(t) + F_{kq}(t)], \tag{15}$$

where $P_1 = \chi\varrho_+$, $P_2 = \chi\varrho_-$, $P_3 = T$, $\widehat{\omega}_1 = 2\Omega + 2\chi(\frac{1}{2} + b^{\dagger}b)$, $\widehat{\omega}_2 = -\widehat{\omega}_1$, $\widehat{\omega}_3 = 0$, $F_{kq}^{\dagger}(t) = c_{Sk}^{\dagger}c_{Dq+}e^{i(\omega_{Sk}-\omega_{Dk})}$, and $F_{kq}(t) = c_{Dq}^{\dagger}c_{Sk}e^{-i(\omega_{Sk}-\omega_{Dk})}$. Applying the Born-Markov approximation and tracing over the degrees of freedom of the QPC, quantum dynamics of the NAMR-DQD system are governed by

$$\dot{\rho}^I(t) = \mathrm{Tr}_{S,D}\Big\{ -i[H_I(t), \rho_{\mathrm{tot}}(0)] - \int_0^{\infty} [H_I(t), [H_I(t'), \rho_{\mathrm{tot}}(t)]]\Big\}. \tag{16}$$

Here, $\rho_{\mathrm{tot}}(t)$ is the density operator of the whole system including the QPC as well. Substituting H_I from Eq. (13) into Eq. (16) and converting the resulting equation into the Schrödinger picture, we obtain the master equation,

$$\dot{\rho}(t) = \mathcal{L}\rho(t) = -i[H_{\mathrm{DQD}}, \rho(t)] + \mathcal{L}_d\rho(t) + \gamma_d\mathcal{D}[\varrho_-]\rho(t), \tag{17}$$

with

$$\mathcal{L}_d\rho(t) = \left\{ \sum_{i=1}^{3} \mathcal{D}[P_i]\rho(t) + \sum_{i=1}^{3}\sum_{j=1\,(j\neq i)}^{3} \mathcal{D}[P_i, P_j]\rho(t) \right\} \times 2\pi g_S g_D \zeta^2 [\Theta(eV_{\mathrm{QPC}} - \omega_i) + \Theta(-eV_{\mathrm{QPC}} - \omega_i)], \tag{18}$$

where $\Theta(x) = (|x| + x)/2$ and $g_{S,D}$ denotes the density of states in the source and drain reservoirs of the QPC, which has a bias voltage V_{QPC}. ω_i is the eigenvalue of the operator $\widehat{\omega}_i$ with the NAMR in the $|n\rangle$ state. Here, for simplicity, the temperatures of the reservoirs in the DQD-QPC system (instead of the temperature T_m of the NAMR) are chosen to be $T = 0$ K because related quantum-dot experiments are performed at extremely low temperatures (see, e.g., Ref. 20). The superoperator $\mathcal{D}$, acting on any single or double operator, is defined as

$$\mathcal{D}[A]\rho \equiv A\rho A^{\dagger} - \tfrac{1}{2}A^{\dagger}A\rho - \tfrac{1}{2}\rho A^{\dagger}A, \tag{19}$$

$$\mathcal{D}[A,B]\rho \equiv \tfrac{1}{2}(A\rho B^{\dagger} + B\rho A^{\dagger} - B^{\dagger}A\rho - \rho A^{\dagger}B). \tag{20}$$

To account for the coupling of the DQD to other degrees of freedom, such as hyperfine interactions and electron-phonon couplings, we have phenomenologically included an additional relaxation term [the third term on the right-hand side of Eq. (17)] describing transitions from excited state $|e\rangle$ to ground state $|g\rangle$.[21] In the strong dispersive regime, as we have mentioned before, the phonon in the NAMR neither is absorbed nor induces any transitions in the DQD and, hence, does not change the occupation probability of the DQD. Instead, the occupation state of the DQD is only affected by the backaction of the QPC and the phenomenological relaxation term.

In the basis $\{|e,n\rangle, |g,n\rangle\}$ of the coupled NAMR-DQD system, we obtain the following evolution equations for the reduced density matrix elements:

$$\dot{\rho}_{en,en} = \gamma_+\rho_{gn,gn} - (\gamma_- + \gamma_d)\rho_{en,en}, \tag{21}$$

$$\dot{\rho}_{gn,gn} = -\gamma_+\rho_{gn,gn} + (\gamma_- + \gamma_d)\rho_{en,en}, \tag{22}$$

$$\dot{\rho}_{en,gn} = -i\delta_n\rho_{en,gn} - \gamma_1(\rho_{en,gn} - \rho_{gn,en}) - \tfrac{1}{2}\gamma_d\rho_{en,gn}, \tag{23}$$

$$\dot{\rho}_{gn,en} = i\delta_n\rho_{gn,en} + \gamma_1(\rho_{en,gn} - \rho_{gn,en}) - \tfrac{1}{2}\gamma_d\rho_{gn,en}. \tag{24}$$

Assuming $eV_{\mathrm{QPC}} > \delta_n > 0$, the QPC-induced relaxation and excitation rates between the ground state and the excited state of the DQD are defined as $\gamma_+ = \gamma_1(1 - \lambda_n)$, $\gamma_- = \gamma_1(1 + \lambda_n)$, where $\gamma_1 = 2\pi g_S g_D \chi^2 eV_{\mathrm{QPC}}$ and $\lambda_n = \delta_n/eV_{\mathrm{QPC}}$. Since the decay rate of the NAMR is much smaller than that of the DQD, dissipations of the NAMR are neglected (see further discussions below). In Eqs. (21)–(24), the reduced density matrix element $\rho_{in,in}(i = g,e)$ gives the occupation probability of state $|i,n\rangle$ of the coupled NAMR-DQD system, whereas $\rho_{in,jn}$ $(i \neq j)$ describes the quantum coherence between states $|i,n\rangle$ and $|j,n\rangle$. Equations of motion for other elements, e.g., $\rho_{in,jn'}$ $(n \neq n')$, which are decoupled from those considered here, are not shown. Using the normalization condition $p_n = \rho_{gn,gn} + \rho_{en,en}$, the solutions to the equations above are obtained as

$$\rho_{en,en}(t) = \left[\rho_{en,en}(0) - \frac{\gamma_+}{2\gamma_0}p_n\right]e^{-2\gamma_0 t} + \frac{\gamma_+}{2\gamma_0}p_n, \tag{25}$$

$$\rho_{gn,gn}(t) = \left[\rho_{gn,gn}(0) - \frac{\gamma_- + \gamma_d}{2\gamma_0}p_n\right]e^{-2\gamma_0 t} + \frac{\gamma_- + \gamma_d}{2\gamma_0}p_n, \tag{26}$$

$$\rho_{en,gn}(t) = e^{-\gamma_0 t}\Big[\cos(\nu_n t)\rho_{en,gn}(0) + \sin(\nu_n t) \times \frac{\gamma_1\rho_{gn,en}(0) - i\delta_n\rho_{en,gn}(0)}{\sqrt{\delta_n^2 - \gamma_1^2}}\Big], \tag{27}$$

$$\rho_{gn,en}(t) = e^{-\gamma_0 t}\Big[\cos(\nu_n t)\rho_{gn,en}(0) + \sin(\nu_n t) \times \frac{\gamma_1\rho_{en,gn}(0) + i\delta_n\rho_{gn,en}(0)}{\sqrt{\delta_n^2 - \gamma_1^2}}\Big], \quad (28)$$

where

$$\gamma_0 = \gamma_1 + \frac{\gamma_d}{2}, \quad (29)$$

$$\nu_n = \sqrt{\delta_n^2 - \gamma_1^2}, \quad (30)$$

and p_n is the probability that the NAMR is in state $|n\rangle$. In the calculation, we have assumed $0 < \gamma_1 < \delta_n$ (see typical parameters listed in Sec. V A).

V. CURRENT CORRELATION SPECTRUM OF THE QPC

The dc current through the QPC is given by[22]

$$I(t) = I_l\rho_{11}(t) + I_r\rho_{22}(t), \quad (31)$$

where $I_l = eD$ and $I_r = eD'$ are the currents through the QPC when dots 1 and 2, respectively, are occupied.[22] Here, $D = 2\pi g_S g_D(T-\zeta)^2 eV_{\rm QPC}$ and $D' = 2\pi g_S g_D(T+\zeta)^2 eV_{\rm QPC}$ are the corresponding rates of electron tunneling through the QPC, which follows from Eq. (7). Using $\rho_{11} + \rho_{22} = 1$, one can define the current operator as

$$\hat{I}(t) = I_0 - I_1\sigma_z, \quad (32)$$

with $I_0 = \frac{e}{2}(D + D')$ and $I_1 = \frac{e}{2}(D - D')$ and $\varrho_x = -\sigma_z$ in the degenerate-state case with $\Delta = 0$. According to the Wiener-Khintchine theorem, when the phonon in the NAMR is in state $|n\rangle$, the QPC current correlation power spectrum $S_n(\omega)$ is given in terms of the two-time correlation function as[19]

$$S_n(\omega) = 2\Re\int_0^{+\infty} d\tau\, e^{i\omega\tau}[\langle\hat{I}(t)\hat{I}(t+\tau)\rangle_n - \langle\hat{I}(t+\tau)\rangle_n\langle\hat{I}(t)\rangle_n]. \quad (33)$$

Substituting Eqs. (25)–(28) and (32) into Eq. (33) and using $S(\omega) = S_0 + \sum_n p_n S_n(\omega)$, we get

$$\frac{S(\omega)}{S_0} = 1 + \frac{2\gamma_1\gamma_2}{\gamma_1+\gamma_2}\sum_n p_n^2\Big\{\frac{\gamma_0}{\gamma_0^2 + (\nu_n-\omega)^2} \times\Big[1 + \frac{\gamma_1}{\gamma_0}\Big(1 + \frac{\omega}{\nu_n}\Big) + \frac{\gamma_+ - \gamma_- - \gamma_d}{2\gamma_0}\frac{\delta_n}{\nu_n}\Big] + \frac{\gamma_0}{\gamma_0^2 + (\nu_n+\omega)^2}\Big[1 + \frac{\gamma_1}{\gamma_0}\Big(1 - \frac{\omega}{\nu_n}\Big) + \frac{\gamma_+ - \gamma_- - \gamma_d}{2\gamma_0}\frac{\delta_n}{\nu_n}\Big]\Big\}. \quad (34)$$

Here, $S_0 = 2eI_0$ is the current-noise background. From Eq. (34), one sees that the current correlation spectrum of the QPC consists of peaks at resonance frequencies $\omega = \pm\nu_n$. These peaks have width γ_0 and heights increasing with the probability p_n. In particular, for small backaction from the QPC, i.e., $\gamma_1 \ll \delta_n$, peaks are located at the resonance point $\omega = \delta_n = 2\Omega + (2n+1)\chi$, admitting a shift $(2n+1)\chi$ inherited from the phonon-number-dependent frequency shift in the DQD as explained above. Thus, one can read out the phonon-number state of the NAMR from these peak shifts in the current correlation spectrum of the QPC.

A. Verification of ground-state cooling of the NAMR

The observation of quantum-mechanical phenomena requires a high frequency and a low temperature for the NAMR (see, e.g., Refs. 5–7) so that $N_{\rm th} \equiv k_{\rm B}T_m/\hbar\omega_m < 1$ or $\langle n\rangle < 0.582$, where $N_{\rm th}$ is the thermal occupation number and $k_{\rm B}$ is the Boltzmann constant. We now assume thermal equilibrium of the NAMR with a probability[19] $p_n \propto e^{-\langle n|H_{\rm NAMR}|n\rangle/k_{\rm B}T}$ for a state $|n\rangle$ so that $p_n = \langle n\rangle^n/(1+\langle n\rangle)^{n+1}$. In general, a state with the average phonon number $\langle n\rangle \ll 1$ (e.g., $\langle n\rangle = 0.01$) implying $p_0 \approx 1$ is considered as a quantum ground state.

By using typical parameters[18,21,23–25] $\omega_m = 2\pi \times 100$, $\Omega = 2\pi \times 200$ MHz, $g = 0.3\omega_m$, $\zeta/T = 0.044$, $\gamma_2 = 0.01\omega_m$, $\gamma_1 = 0.2\gamma_2$, and $\gamma_d = 2\gamma_2$, the current correlation spectrum of the QPC is calculated and is presented in Fig. 2 where only the positive frequency regime is shown. For $\langle n\rangle = 0.02 \ll 0.582$ in the quantum regime [see Fig. 2(a)], there is only a single peak in the spectrum corresponding to the transition frequency between the two eigenstates of the DQD. From Eq. (34), the peak is located at the resonance frequency ν_0 given in Eq. (30). The corresponding probability distribution function p_n is also shown in the right panel of the figures showing the probability of finding the NAMR in state

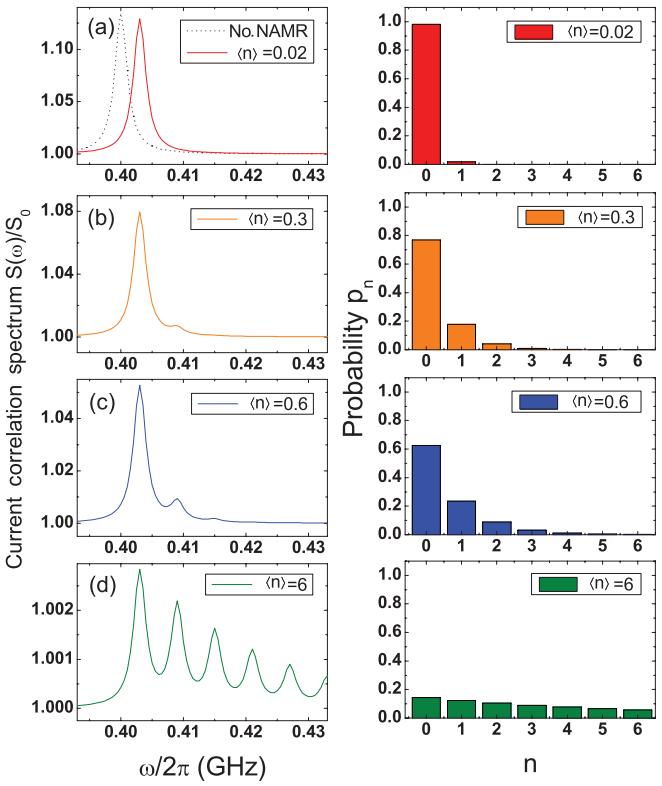

FIG. 2. (Color online) Left panel: Current correlation spectrum of the QPC when the average phonon numbers in the NAMR are (a) $\langle n\rangle = 0.02$, (b) 0.3, (c) 0.6, and (d) 6, respectively, given by the thermal distribution, i.e., $p_n = \langle n\rangle^n/(1+\langle n\rangle)^{n+1}$. Right panel: the corresponding probability of the NAMR in state $|n\rangle$. The coupling strength between the NAMR and the DQD is chosen as $g = 0.3\omega_m$. The other parameters are $\omega_m = 2\pi \times 100$ MHz, $\Omega = 2\omega_m$, $\gamma_2 = 0.01\omega_m$, $\gamma_1 = 0.2\gamma_2$, $\gamma_d = 2\gamma_2$, and $\zeta/T = 0.044$.

$|n\rangle$. This spectrum is nearly indistinguishable from the pure ground state with $\langle n\rangle = 0$. At a higher temperature, other peaks begin to appear in the current correlation spectrum [Fig. 2(b)]. The peak position as given in Eqs. (30) and (34) admits an NAMR-induced shift analogous to an ac Stark shift. In the regime with, e.g., $\langle n\rangle = 0.6$ [Fig. 2(c)] and 6 [Fig. 2(d)], multiple peaks are obtained. As each resonance peak in the spectrum corresponds to a phonon-number state of the NAMR, the relative area under each peak could be used, in principle, to calculate the phonon statistics of the NAMR.

To observe multiple peaks in the correlation spectrum, the separation between two adjacent peaks must be larger than the intrinsic peak width, i.e., $2\chi > \gamma_0$. The ensemble can then be individually resolved, which allows us to detect the phonon number to verify the cooling efficiency of the NAMR. On the contrary, the phonon-number state of the NAMR cannot be measured when $2\chi < \gamma_0$. Indeed, a relatively strong coupling between an NAMR and a quantum dot has been recently demonstrated.[26] Thus, the regime with $2\chi > \gamma_0$ could be achievable. Also, the ground-state cooling of an NAMR coupled to a DQD was proposed.[17] One can then apply the proposed coupled NAMR-DQD system to verify the ground-state cooling of the NAMR. The frequency shifts in the DQD energy levels are also different for the ground and excited states of the NAMR and can then be used to read out the phonon state of the NAMR, which can be different from the phonon statistics in the thermal state discussed above.

Figure 3(a) shows the current correlation spectrum of the QPC when the NAMR is in its ground state with $\langle n\rangle = 0.02$.

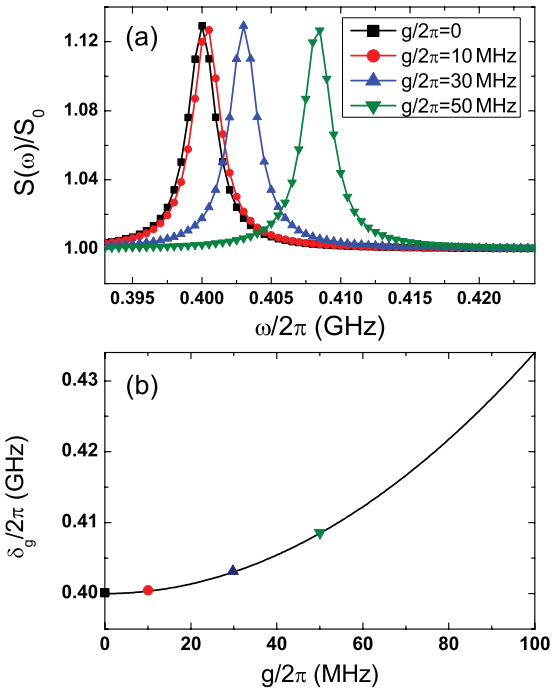

FIG. 3. (Color online) (a) Current correlation spectrum of the QPC when the NAMR is in the ground state and the coupling strengths g between the NAMR and the DQD are 0 (black squares), 10 MHz (red circles), 30 MHz (blue upper triangles), and 50 MHz (olive lower triangles), respectively. (b) Frequency shift δ_g as a function of the coupling strength g when the NAMR is in the ground state. Other parameters are the same as those in Fig. 2.

If the NAMR and the DQD are decoupled, i.e., $g = 0$, the frequency corresponding to the peak position is about $2\pi \times 0.4$ GHz, which is the transition frequency 2Ω between the two eigenstates of the DQD. By increasing the coupling strength g, we find that the peak shifts to the right, while the linewidth as well as the amplitude are unchanged. This suggests that the energy levels of the DQD are shifted so that the energy splitting is widened under the effect of the NAMR. However, these changes do not involve the absorption of any NAMR phonon. As demonstrated in Fig. 3(b), the frequency shift increases with the square of the coupling strength between the DQD and the NAMR, consistent with $\chi = g^2/\delta$ in Eq. (10).

B. QPC-induced backaction in the current correlation spectrum of the QPC

The backaction on the DQD due to measurement by the QPC is illustrated in Fig. 4 when the NAMR is practically in its ground state with $\langle n\rangle = 0.02$. There is no backaction effect when the bias voltage $V_{\rm QPC}$ across the QPC is less than the energy difference between the two DQD eigenstates,[21] i.e., $eV_{\rm QPC} < \delta_0$. At $eV_{\rm QPC} = 2\pi \times 0.5$ GHz $> \delta_0$, for example, a single peak located at $\omega \sim 2\pi \times 0.4$ GHz appears. When $V_{\rm QPC}$ is increased, we find that the linewidth of the spectrum becomes broadened, which results from $\gamma_0 = \gamma_1 + \gamma_d/2$ where γ_1 is proportional to the bias voltage. Physically, the broadening results from more frequent state transitions in the DQD induced by the backaction from the QPC when a larger bias voltage is applied across the QPC.

Dissipations in the NAMR due to the environment have been neglected in our analysis. Dissipation in an NAMR (see Ref. 27) can be expressed as $\gamma_m = \omega_m/Q$ with a quality factor Q. However, even for the NAMR-DQD coupling discussed above (e.g., $2\pi \times 30$ MHz), the dissipation of the NAMR is still very small: $\gamma_m/g \sim 10^{-4}$ for an experimentally achievable quality factor[26] $Q = 10^5$. This justifies neglecting the dissipations of the NAMR due to other environmental effects in our calculations.

For a QPC, a Kondo-like model was proposed in Ref. 28, which is similar to the Kondo problem in a single quantum dot

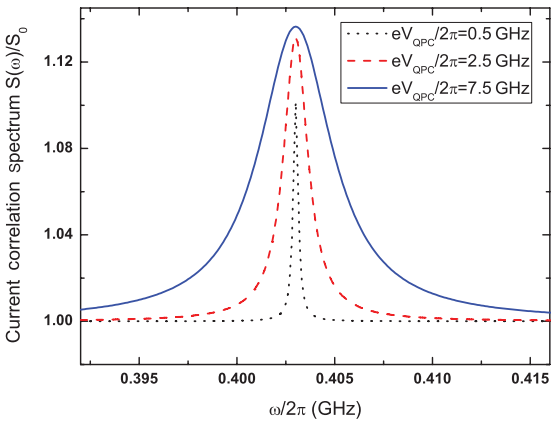

FIG. 4. (Color online) Current correlation spectrum of the QPC at various voltage biases $V_{\rm QPC}$ of the QPC when the NAMR is approximately in the ground state, i.e., $\langle n\rangle = 0.02$. Other parameters are the same as those in Fig. 2.

coupled to two leads where the spin degree of freedom plays an important role. Here, as in Refs. 22 and 29, the QPC we used is simply modeled as a tunneling junction, and the spin degree of freedom does not affect its performance. In addition, it should be noted that the Kondo effect in the DQD can be avoided here. In fact, the present setup involves no reservoirs (leads) coupled to the DQD because the coupling between the DQD and the reservoirs is tuned to zero or is negligibly small. Nevertheless, the Kondo effect in a DQD needs a strong coupling between the DQD and the reservoirs in addition to other requirements.

In practice, there are finite cross-capacitive couplings among various gate electrodes, which affect the whole system. However, because the coupling between the NAMR and the DQD is in the dispersive regime, the effect of the NAMR on varying the parameters of the DQD is small. As for the cross-capacitive couplings in the DQD system, the experiment in Ref. 30 showed that the effect of the cross-capacitive couplings can be canceled by adjusting the plunger voltage of the detector during sweeps of the DQD plunger voltages. In our proposed setup in Fig. 1(b), more gate electrodes are introduced. This will enhance the tunability of the DQD system to achieve the needed parameters of the system.

VI. CONCLUSIONS

We have proposed an approach to study quantum behaviors of an NAMR by coupling it indirectly to a QPC as a charge detector via a DQD serving as a quantum transducer. By detecting the current correlation spectrum of the charge detector, quantum behaviors of the NAMR can be observed. It provides interesting insight on the quantum system as well as dynamics of these backaction effects induced by an act of measurement, which necessarily perturbs the system being measured. More importantly, the cooling of the NAMR down to the quantum regime can be verified. In the quantum regime, NAMR-phonon-induced shifts (an analog to the Stark shift) of DQD energy levels as well as their relations with coupling strength between the NAMR and the DQD are demonstrated. Backaction effects from the charge detector are also explained.

ACKNOWLEDGMENTS

This work was supported by the National Basic Research Program of China Grant No. 2009CB929300, the National Natural Science Foundation of China Grant No. 91121015, and the Research Grant Council of Hong Kong SAR under Project No. 5009/08P.

*jqyou@fudan.edu.cn

[1] M. P. Blencowe, Phys. Rep. **395**, 159 (2004).
[2] K. C. Schwab and M. L. Roukes, Phys. Today **58**(7), 36 (2005).
[3] A. Cho, Science **299**, 36 (2003).
[4] C. A. Regal and K. W. Lehnert, J. Phys.: Conf. Ser. **264**, 012025 (2011).
[5] A. Gaidarzhy, G. Zolfagharkhani, R. L. Badzey, and P. Mohanty, Phys. Rev. Lett. **94**, 030402 (2005); **95**, 248902 (2005); K. C. Schwab, M. P. Blencowe, M. L. Roukes, A. N. Cleland, S. M. Girvin, G. J. Milburn, and K. L. Ekinci, *ibid.* **95**, 248901 (2005).
[6] R. L. Badzey and P. Mohanty, Nature (London) **437**, 995 (2005).
[7] W. K. Hensinger, D. W. Utami, H. S. Goan, K. Schwab, C. Monroe, and G. J. Milburn, Phys. Rev. A **72**, 041405(R) (2005).
[8] M. D. LaHaye, O. Buu, B. Camarota, and K. C. Schwab, Science **304**, 74 (2004).
[9] X. M. H. Huang, C. A. Zorman, M. Mehregany, and M. L. Roukes, Nature (London) **421**, 496 (2003).
[10] R. G. Knobel and A. N. Cleland, Nature (London) **424**, 291 (2003).
[11] A. N. Cleland, J. S. Aldridge, D. C. Driscoll, and A. C. Gossard, Appl. Phys. Lett. **81**, 1699 (2002).
[12] W. Marshall, C. Simon, R. Penrose, and D. Bouwmeester, Phys. Rev. Lett. **91**, 130401 (2003).
[13] M. F. Bocko and R. Onofrio, Rev. Mod. Phys. **68**, 755 (1996).
[14] J. D. Teufel, T. Donner, Dale Li, J. W. Harlow, M. S. Allman, K. Cicak, A. J. Sirois, J. D. Whittaker, K. W. Lehnert, and R. W. Simmonds, Nature (London) **475**, 359 (2011).
[15] M. R. Geller and A. N. Cleland, Phys. Rev. A **71**, 032311 (2005).
[16] L. F. Wei, Y. X. Liu, C. P. Sun, and F. Nori, Phys. Rev. Lett. **97**, 237201 (2006).
[17] S. H. Ouyang, J. Q. You, and F. Nori, Phys. Rev. B **79**, 075304 (2009).
[18] N. Lambert and F. Nori, Phys. Rev. B **78**, 214302 (2008).
[19] M. O. Scully and M. S. Zubairy, *Quantum Optics* (Cambridge University Press, Cambridge, UK, 1997).
[20] S. Gustavsson, M. Studer, R. Leturcq, T. Ihn, K. Ensslin, D. C. Driscoll, and A. C. Gossard, Phys. Rev. Lett. **99**, 206804 (2007).
[21] S. H. Ouyang, C. H. Lam, and J. Q. You, Phys. Rev. B **81**, 075301 (2010).
[22] S. A. Gurvitz, Phys. Rev. B **56**, 15215 (1997).
[23] W. G. van der Wiel, S. De Franceschi, J. M. Elzerman, T. Fujisawa, S. Tarucha, and L. P. Kouwenhoven, Rev. Mod. Phys. **75**, 1 (2003).
[24] T. F. Li, Y. A. Pashkin, O. Astafiev, Y. Nakamura, J. S. Tsai, and H. Im, Appl. Phys. Lett. **92**, 043112 (2008).
[25] L. M. K. Vandersypen, J. M. Elzerman, R. N. Schouten, L. H. W. van Beveren, R. Hanson, and L. P. Kouwenhoven, Appl. Phys. Lett. **85**, 4394 (2004).
[26] A. K. Hüttel, G. A. Steele, B. Witkamp, M. Poot, L. P. Kouwenhoven, and H. S. J. van der Zant, Nano Lett. **9**, 2547 (2009).
[27] J. Tamayo, J. Appl. Phys. **97**, 044903 (2005); A. N. Cleland and M. L. Roukes, *ibid.* **92**, 2758 (2002).
[28] Y. Meir, K. Hirose, and N. S. Wingreen, Phys. Rev. Lett. **89**, 196802 (2002).
[29] H. A. Engel, V. N. Golovach, D. Loss, L. M. K. Vandersypen, J. M. Elzerman, R. Hanson, and L. P. Kouwenhoven, Phys. Rev. Lett. **93**, 106804 (2004).
[30] Y. Hu, H. O. H. Churchill, D. J. Reilly, J. Xiang, C. M. Lieber, and C. M. Marcus, Nature Nanotech. **2**, 622 (2007).